

A multifrequency study of possible relic lobes in giant radio sources

Sagar Godambe^{1,2*}, C. Konar³, D.J. Saikia¹ and Paul J. Wiita^{4,5}

¹ National Centre for Radio Astrophysics, Tata Institute of Fundamental Research, Post Bag 3, Ganeshkhind, Pune 411007, India

² Department of Physics, The University of Utah, Salt Lake City, UT 84112-0830, USA

³ Inter-University Centre for Astronomy and Astrophysics, Post Bag 4, Ganeshkhind, Pune 411007, India

⁴ Department of Physics and Astronomy, Georgia State University, PO Box 4106, Atlanta, Georgia 30302-4106, USA

⁵ School of Natural Sciences, Institute for Advanced Study, Princeton, New Jersey, 08540, USA

Accepted. Received

ABSTRACT

We present low-frequency observations with the Giant Metrewave Radio Telescope (GMRT) of three giant radio sources (GRSs, J0139+3957, J0200+4049 and J0807+7400) with relaxed diffuse lobes which show no hotspots and no evidence of jets. The largest of these three, J0200+4049, exhibits a depression in the centre of the western lobe, while J0139+3957 and J0807+7400 have been suggested earlier by Klein et al. and Lara et al. respectively to be relic radio sources. We estimate the ages of the lobes. We also present Very Large Array (VLA) observations of the core of J0807+7400, and determine the core radio spectra for all three sources. Although the radio cores suggest that the sources are currently active, we explore the possibility that the lobes in these sources are due to an earlier cycle of activity.

Key words: galaxies: active – galaxies: individual (J0139+3957, J0200+4049 and J0807+7400) – galaxies: nuclei – radio continuum: galaxies

1 INTRODUCTION

Giant radio sources (GRSs) are defined to be those which have a projected linear size $\gtrsim 1$ Mpc ($H_0=71$ km s⁻¹ Mpc⁻¹, $\Omega_m=0.27$, $\Omega_{vac}=0.73$, Spergel et al. 2003), and provide useful insights towards understanding the late stages of evolution of radio sources and probing the external environment on Mpc scales at different redshifts (e.g. Gopal-Krishna, Wiita & Saripalli 1989; Subrahmanyan & Saripalli 1993; Subrahmanyan, Saripalli & Hunstead 1996; Mack et al. 1998; Ishwara-Chandra & Saikia 1999; Kaiser & Alexander 1999; Blundell, Rawlings & Willott 1999 and references therein; Schoenmakers et al. 2000, 2001; Konar et al. 2004, 2008; Machalski et al. 2007, 2008; Jamrozy et al. 2008).

There have been many attempts to determine the ages of double-lobed radio sources including the GRSs. Most lobes of GRSs exhibit a steepening in spectral index from the outer peaks towards the nuclear region, allowing an estimate of the spectral age, similar to what has been done for double-lobed radio sources of smaller dimensions. For a sample of GRSs observed with the Giant Metrewave Radio

Telescope (GMRT) and the Very Large Array (VLA), Jamrozy et al. (2008) have estimated their median age to be ~ 20 Myr while their median size is ~ 1300 kpc. The spectral age is likely to be a lower limit since the radio emission is often not seen all the way to the nuclear region, and there could also be re-acceleration of particles in the lobes. For the smaller sources a large number of studies of spectral ages have been made. For example, for a sample of 3CR sources with a median size of 342 kpc studied by Leahy, Muxlow & Stephens (1989) using the Multi-Element Radio Linked Interferometer Network (MERLIN) at 151 MHz and the VLA at 1500 MHz, the spectral age was found to have a median value of ~ 8 Myr. Similar gradients in spectral index across the lobes have also been seen in smaller sources such as those studied by Liu, Pooley & Riley (1992) which have a median linear size of 103 kpc and a median age of ~ 1.7 Myr. There is a clear trend for the spectral age to increase with size, which is broadly consistent with the expectations of dynamical models of the propagation of jets in an external medium (e.g. Falle 1991; Kaiser & Alexander 1997; Jeyakumar et al. 2005 and references therein).

In the course of our study of GRSs, a number of these objects appeared to have diffuse lobes of emission without any prominent peaks of emission towards the outer edges of the lobes. Unlike Fanaroff-Riley Class I sources, these

* E-mail: sagar.godambe@gmail.com (SG); chiranjib@iucaa.ernet.in (CK); djs@ncra.tifr.res.in (DJS); wiita@chara.gsu.edu (PJW)

Table 1. Observing log

Telescope	Array Conf.	Obs. Freq. MHz	Sources	Obs. Date
(1)	(2)	(3)	(4)	(5)
GMRT		239	J0139+3957	2007 Jun 02
GMRT		334	J0139+3957	2005 Jan 28
GMRT		605	J0139+3957	2007 Jun 02
GMRT		1287	J0139+3957	2003 Aug 19
VLA ^a	D	4841	J0139+3957	2000 Jul 24
GMRT		239	J0200+4049	2007 Dec 29
GMRT		333	J0200+4049	2004 Dec 25
GMRT		605	J0200+4049	2007 Dec 29
GMRT		1289	J0200+4049	2004 Nov 25
GMRT		239	J0807+7400	2005 Jan 07
GMRT		334	J0807+7400	2004 Dec 07
GMRT		605	J0807+7400	2005 Jan 07
GMRT		1289	J0807+7400	2005 Jan 17
VLA ^b	B	1385	J0807+7400	1995 Nov 19
VLA ^b	D	1435	J0807+7400	1993 Nov 01
VLA ^b	C	1685	J0807+7400	1996 Feb 19
VLA ^b	C	4860	J0807+7400	1996 Feb 19

^a Image published by Konar et al. (2004).

^b Archival data from the VLA.

do not have any jets and the radio emission could be from relic lobes. We have chosen three of these sources, namely J0139+3957, J0200+4049 and J0807+7400, for a detailed investigation using the GMRT. Two of these, J0139+3957 and J0807+7400, have been suggested earlier to be relic radio sources by Klein et al. (1995) and Lara et al. (2001) respectively. In this paper we present the results of multifrequency observations of these three sources at low frequencies with the GMRT, attempt to estimate their spectral ages and explore the possibility that these lobes might be relics from an earlier cycle of activity. We also present the core flux densities of J0807+7400 from archival VLA data, and the core spectra of the three sources.

2 OBSERVATIONS AND ANALYSES

Both the GMRT and the VLA observations were made in the standard fashion, with each target source observation interspersed with observations of the phase calibrator. The primary flux density calibrator was any one of 3C48, 3C147 and 3C286 with all flux densities being on the scale of Baars et al. (1977). The total observing time on each source is a few hours for the GMRT observations while for the VLA observations the time on source ranges up to 10 minutes. All the data were analysed in the standard fashion using the NRAO AIPS package. All the data were self calibrated to produce the best possible images.

The observing log for both the GMRT and the VLA observations is given in Table 1 which is arranged as follows. Columns 1 and 2 show the name of the telescope and the array configuration for the VLA observations; column 3 shows the frequency of the observations in MHz, while columns 4 and 5 list the sources observed and the dates of the observations, respectively.

3 OBSERVATIONAL RESULTS

The GMRT images of the three sources, J0139+3957, J0200+4049 and J0807+7400, at the different frequencies are presented in Figs. 1, 2 and 3 respectively, while the observational parameters and some of the observed properties are presented in Table 2, which is arranged as follows. Column 1: Name of the source; column 2: frequency of observations in units of MHz; columns 3-5: the major and minor axes of the restoring beam in arcsec and its position angle (PA) in degrees; column 6: the rms noise in units of mJy beam⁻¹; column 7: the integrated flux density of the source in mJy estimated by specifying an area enclosing the entire source. We examined the change in flux density by specifying different areas and found the difference to be within a few per cent. The flux densities at different frequencies have been estimated over similar areas. Columns 8, 11 and 14: component designation, where W, C and E denote the western, core and eastern components respectively; columns 9 and 10, 12 and 13, and 15 and 16: the peak and total flux densities of each of the components in units of mJy beam⁻¹ and mJy respectively. The superscript *g* indicates that the flux densities have been estimated from a two-dimensional Gaussian fit to the core component.

4 DISCUSSION AND RESULTS

The integrated flux densities of the sources from our measurements as well as those from the literature are listed in Table 3, which is self-explanatory, while some of the physical properties of the sources are listed in Table 4 which is arranged as follows. Column 1: source name; Column 2: redshift; columns 3 and 4: the largest angular size in arcsec and the corresponding projected linear size in kpc; column 5: the luminosity at 1.4 GHz in logarithmic units of W Hz⁻¹; columns 6 and 10: lobe designation where W and E denote the western and eastern lobes respectively; columns 7 and 11: break frequency, ν_B , with errors in units of GHz; columns 8 and 12: magnetic field, B_{eq} , in units of nT; columns 9 and 13: spectral ages of the lobes with errors in units of Myr.

For all the lobes listed in Table 2 we have fitted the observed spectra for the Jaffe & Perola (1973, JP) model using the SYNAGE package (Murgia 1996; Murgia et al. 1999) to estimate the break frequency listed in columns 7 and 11 of Table 4. Since the integrated spectra at low frequencies are usually determined from a larger number of measurements than those of the individual lobes of emission, we have fixed the value of α_{inj} from a fit to the integrated spectrum using the SYNAGE package. However, because of the very diffuse extended emission in these sources, several measurements even at low frequencies appear to have missed a significant amount of the total flux density. The highly discrepant measurements have not been used in the final fits for estimating α_{inj} , where the typical error in α_{inj} is within about ± 0.1 . For a sample of GRSs studied earlier (Konar et al. 2008; Jamroz et al. 2008), the values of α_{inj} estimated for the lobes when possible are similar, within the uncertainties, to those estimated from the integrated spectra. Therefore this procedure has been adopted for all the three sources considered here. We also examined the spectral index images of the

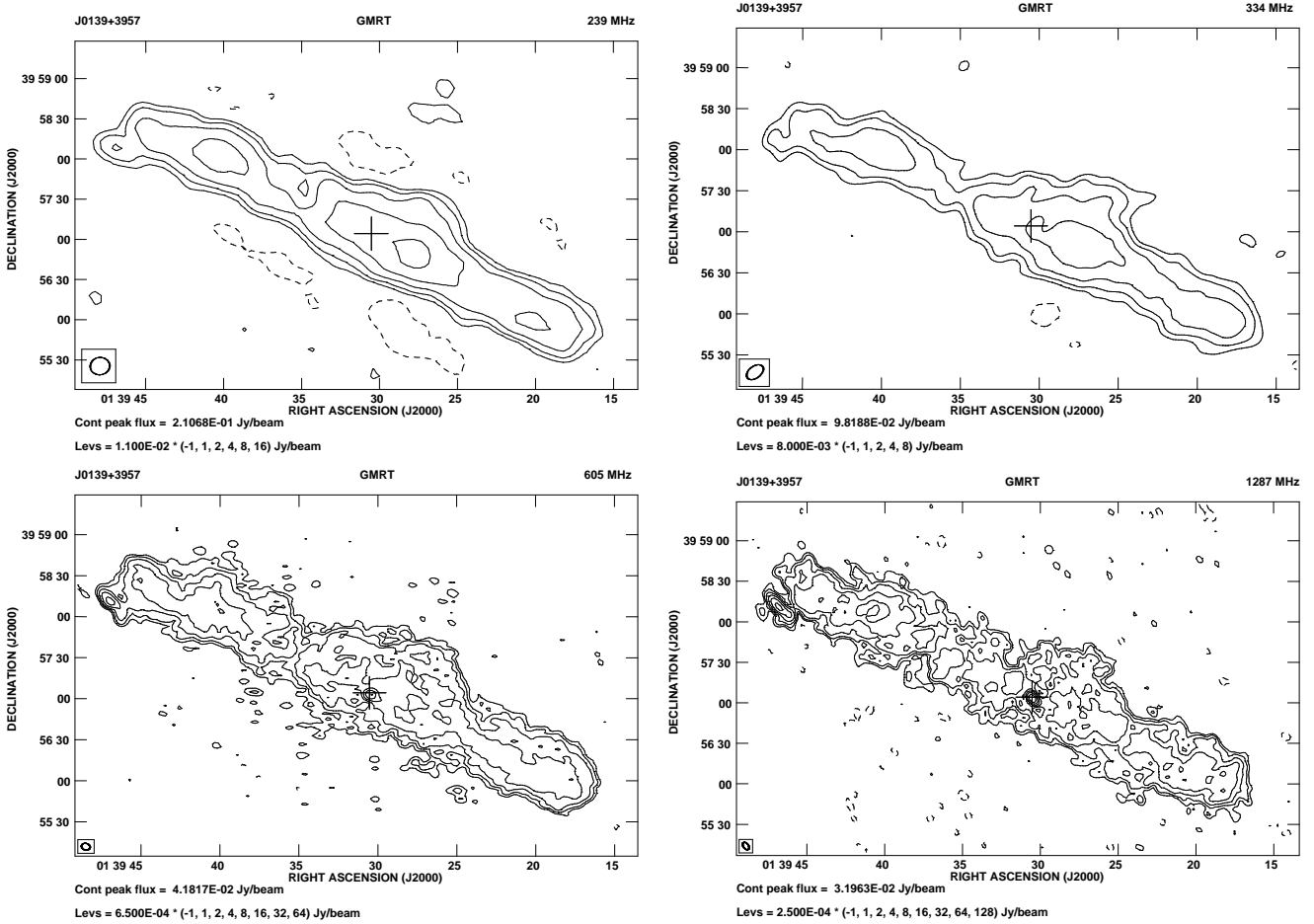


Figure 1. GMRT images of J0139+3957 at 239, 334, 605 and 1287 MHz. The image at 1287 MHz has been reproduced from Konar et al. (2004). In this figure as well as in all the other images of the sources, the peak brightness and the contour levels in units of Jy beam^{-1} are given below each image. In all the images the restoring beams are indicated by ellipses; the values are those listed in Table 2 unless mentioned otherwise in the caption. The + sign indicates the position of the optical host galaxy.

Table 2. The observational parameters and observed properties of the sources from the GMRT images.

Source	Freq. MHz	Beam size			rms	S_I	C_p	S_p	S_t	C_p	S_p	S_t	C_p	S_p	S_t
		"	"	"	mJy	mJy	mJy	mJy		mJy	mJy		mJy	mJy	
(1)	(2)	(3)	(4)	(5)	(6)	(7)	(8)	(9)	(10)	(11)	(12)	(13)	(14)	(15)	(16)
J0139+3957	239	14.3	12.9	278	2.85	6415	W	211	3609				E	143	2728
	334	13.9	8.6	308	2.58	5434	W	103	3403				E	75	2044
	605	6.3	4.9	74	0.16	2643	W	42	1445	C^g	38	74	E	42	1249
	1287	6.2	3.8	37	0.05	1201	W	4.5	600	C^g	34	35	E	10	579
J0200+4049	239	20.5	12.6	58	0.83	9129	W	25	4788				E	25	4543
	333	10.2	8.2	68	0.28	10000	W	8.4	5028	C^g	9.5	14.8	E	8.1	5183
	605	5.4	5.3	88	0.13	5014	W	2.3	2733	C^g	8.4	9.6	E	2.5	2384
J0807+7400	1289	3.7	2.5	316	0.12					C	6.4	8.9			
	239	41.8	32.0	312	1.5	929	W	74	404				E	80	557
	334	13.2	9.5	63	0.32	937	W	6.2	396	C^g	40	45	E	8.8	493
	605	7.0	5.7	346	0.08	433	W	14	192	C^g	19	22	E	20	238
	1289	9.6	9.3	83	0.05	169	W	11	81	C^g	8.5	11.6	E	7.4	87

C: Values of core flux densities listed here have been estimated from images with the resolutions given here. Estimates by mapping with a lower uv-cut-off are listed later, along with values from the literature.

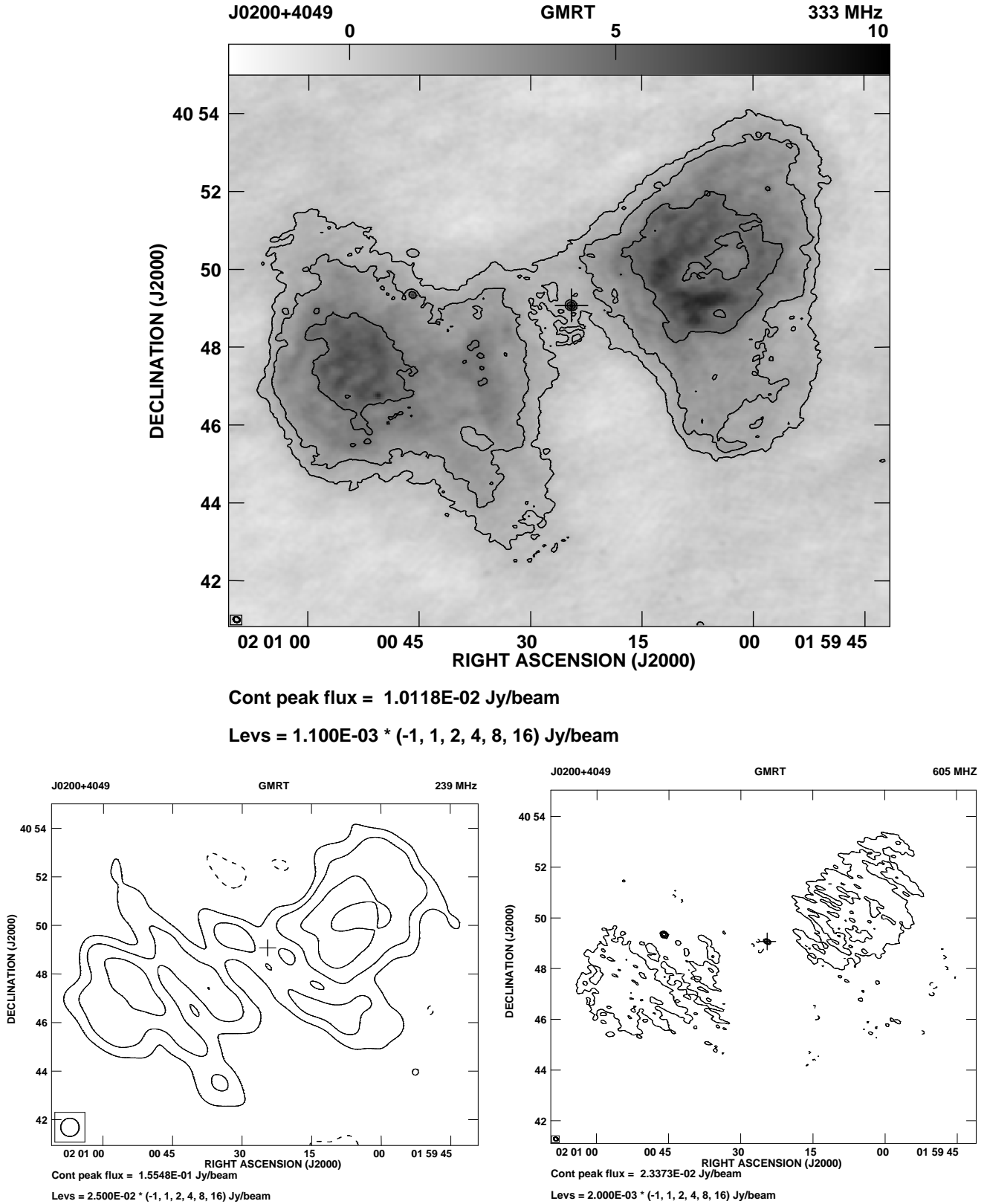


Figure 2. GMRT image of J0200+4049 at 333 MHz is shown in the upper panel. The 239-MHz image convolved to a resolution of 45 arcsec, and the 605-MHz image convolved to the resolution of the 333-MHz image are shown in the lower panels.

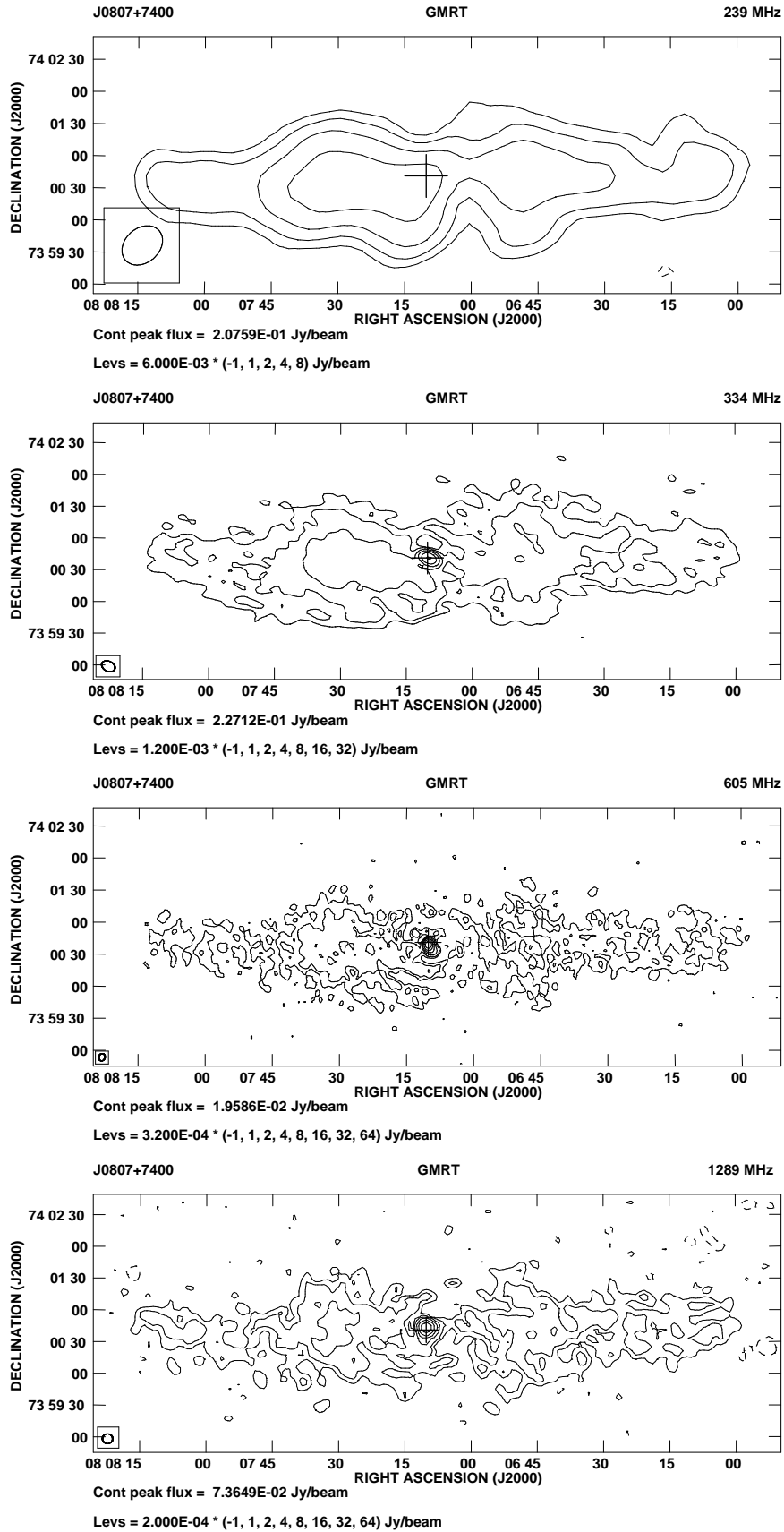


Figure 3. GMRT images of J0807+7400 at 239, 334, 605 and 1289 MHz.

Table 3. The total flux densities

Source	Freq.	Flux density	Error	References
(1)	(2)	(3)	(4)	(5)
J0139+3957	26.3	64960	6086	9
	74	17821	2673	1
	151	10800	756	10
	178	4773	596	11
	239	6415	962	P
	325	4750	100	15
	334	5434	815	P
	408	3890	195	12
	605	2643	264	P
	1287	1201	120	P
	1400	798	16	15
	1400	802	80	2
	1460	1037	104	3
	4841	203	20	4
	4850	262	30	15
	10450	106	4	15
	10550	115	7	16, 18
J0200+4049	26.3	52780	6000	9
	74	5519	828	1
	151	12080	846	10
	178	2997	450	12
	239	9129	1369	P
	325	2980	80	15
	327	4360	184	17
	333	10000	1500	P
	408	4390	219	3
	605	5014	501	P
	1400	292	29	2
	1400	220	10	17
	1400	1261	126	6
	1460	1359	136	3
	4850	180	27	7
	4850	292	35	15
	4850	418	10	17
10450	95	11	15	
10550	95	2	17, 18	
J0807+7400	38	3300	900	13
	151	1220	90	14
	239	929	139	P
	334	937	141	P
	605	433	43	P
	1289	169	17	P
	1400	155	16	2
	1465	152	15	5
	4850	46	7	8
4850	38	6	7	

P: Present paper 1: VLA Low-frequency Sky Survey (VLSS; <http://lwa.nrl.navy.mil/VLSS>); 2: NRAO VLA Sky Survey (NVSS; Condon et al. 1998); 3: Vigotti et al. 1989; 4: Konar et al. 2004; 5: Lara et al. 2001; 6: White & Becker 1992; 7: Becker, White & Edwards 1991; 8: Gregory & Condon 1991; 9: Viner & Erickson 1975; 10: Hales, Baldwin & Warner 1993; 11: Pilkington & Scott 1965; 12: Gower, Scott & Wills 1967; 13: Hales et al. 1995; 14: Hales et al. 1991; 15: Schoenmakers et al. 2000; 16: Mack et al. 1994; 17: Vigotti et al. 1999; 18: Gregorini et al. 1998.

sources, but due to the large diffuse nature of the lobes and different uv coverages at different frequencies, age estimates using the integrated spectra of the lobes were found to be more reliable. While estimating α_{inj} , the core flux density has been subtracted from the total flux density.

The minimum energy magnetic field has been estimated by integrating the spectrum from a frequency corresponding to a minimum Lorentz factor, $\gamma_{\text{min}} \sim 10$ for the relativistic electrons to an upper limit of 100 GHz, which corresponds to a Lorentz factor ranging from a few times 10^4 to 10^5 depending on the estimated magnetic field strength (see Hardcastle et al. 2004; Croston et al. 2005; Konar et al. 2008). Then, under assumptions that (i) the magnetic field strength in a given lobe is constant throughout the energy-loss process, (ii) the particles injected into the lobe have a constant power-law energy spectrum, and (iii) the time-scale of isotropization of the pitch angles of the particles is short compared with their radiative lifetime, the spectral age, τ_{spec} , has been estimated from

$$\tau_{\text{spec}} = 50.3 \frac{B^{1/2}}{B^2 + B_{\text{IC}}^2} \{\nu_{\text{br}}(1+z)\}^{-1/2} [\text{Myr}], \quad (1)$$

where $B_{\text{IC}} = 0.318(1+z)^2$ is the magnetic field strength equivalent to the cosmic microwave background radiation. Here B , the magnetic field strength of the lobes, and B_{IC} are expressed in units of nT, ν_{br} is the spectral break frequency in GHz above which the radio spectrum steepens from the initial power-law spectral index, α_{inj} , given by $S \propto \nu^{-\alpha_{\text{inj}}}$.

4.1 J0139+3957

The large-scale structure showing the relaxed lobes (Fig. 1) has been reported earlier by a number of authors (e.g. Hine 1979; Vigotti et al. 1989). Klein et al. (1995) presented Efeberg observations of the source and suggested it to be one with possible relic lobes of emission. Konar et al. (2004) reported GMRT and VLA observations at 1287 and 4841 MHz respectively and found that the spectral index of the entire source between 1.3 and 4.8 GHz is 1.34 while that of the core is 0.8. In Fig. 4, we show the fits to the integrated spectra of the entire source as well as the western and eastern lobes using the injection spectral index, $\alpha_{\text{inj}} = 1.00$, determined from the fit to the entire source after subtracting the core flux density. The spectral ages for the western and eastern lobes using our measurements have been found to be 12_{-1}^{+10} and $5.3_{-2.2}^{+29}$ Myr respectively (Table 4).

The existence of a possible steep-spectrum core was noted earlier (e.g. Hine 1979; Klein et al. 1995). Similar-resolution observations of about 5 arcsec between 1.4 and 5 GHz (Fomalont & Bridle 1978; Gregorini et al. 1988; Bondi et al. 1993; Klein et al. 1995) also yield a core spectral index of ~ 0.8 . This is consistent with the 10.6 GHz value of 4 ± 1 mJy (Mack et al. 1994). Saripalli et al. (1997) find the core to be a compact source with a flux density of 20 ± 5 mJy from VLBI observations at 1.67 GHz with a resolution of 25 mas. The core flux densities from our low-frequency measurements, by putting a lower uv limit to minimise any contamination from extended emission, along with values from the literature are listed in Table 5. The spectrum (Fig. 5) shows clearly that while the high frequency spectrum is steep, it flattens below about a GHz.

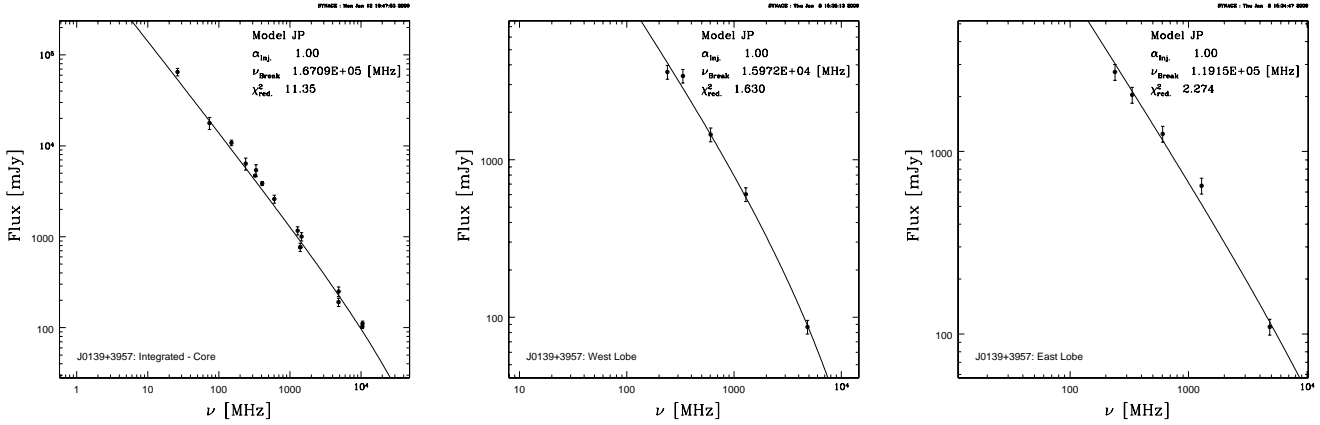


Figure 4. The fits to the spectra of the entire source after subtracting the contribution of the core (left panel), western (middle panel) and eastern (right panel) lobes of J0139+3957 using the SYNAGE package.

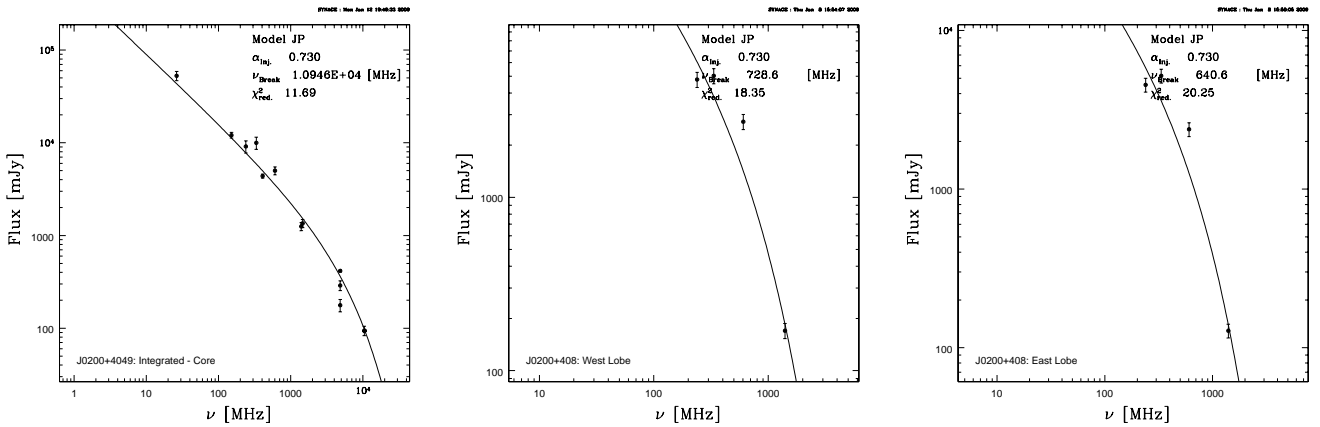


Figure 6. The fits to the spectra of the entire source after subtracting the contribution of the core (left panel), as well as the western (middle panel) and eastern (right panel) lobes of J0200+4049 using the SYNAGE package.

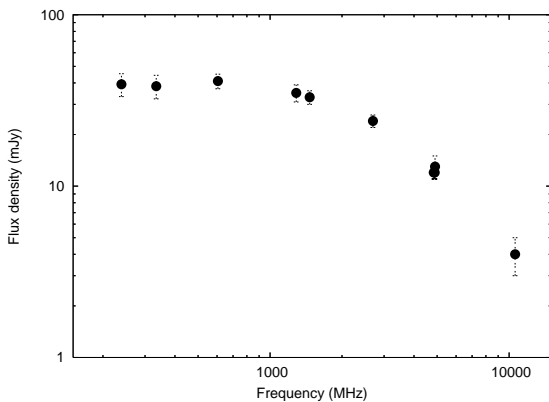


Figure 5. The spectrum of the radio core of J0139+3957.

4.2 J0200+4049

The double lobed structure has been imaged earlier by a number of authors (Vigotti et al. 1989; Gregorini et al. 1988; Schoenmakers et al. 2000), and some of the diffuse emission is also visible in the NVSS image reproduced by Konar et al.

(2004). The latter also report the detection of a radio core at 4.8 GHz with a flux density of 2.6 mJy, and a compact component to the east which is coincident with a faint galaxy seen in the Digital Sky Survey (DSS) image. Our images (Fig. 2) show evidence of a depression in the centre of the western lobe, which is clearly seen in the 333-MHz image. It is also seen at 239 MHz where the data is of poorer quality, and at 605 MHz which require more short-spacing data to produce a better image. The GMRT image at 1289 MHz is not shown here since only the core and the unrelated compact source to the east (see Konar et al. 2004) were visible.

The flux density of the source appears to have been under-estimated in the 74-MHz VLSS image and at 178 MHz in the 4C survey, possibly due to the large extent of the diffuse low-brightness lobes of emission. The values at these frequencies lie significantly below the fit to the integrated spectrum (Fig. 6). For example the flux density at 178 MHz is only ~ 3 Jy while it has been estimated to be approximately 12 Jy at 151 MHz. The flux density values at 74 and 178 MHz have not been considered in the fit to the integrated spectrum of the source. The injection spectral index has been estimated to be 0.73. The spectral ages estimated for the western and eastern lobes using our mea-

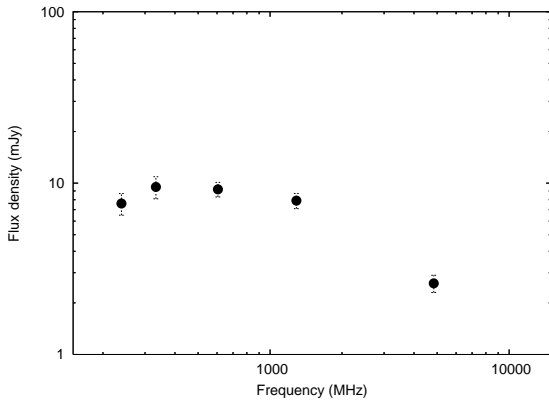
Table 4. Physical properties of the sources

Source	Redshift	LAS	l	$P_{1.4}$	Cmp.	ν_B	B_{eq}	Spec. age	Cmp.	ν_B	B_{eq}	Spec. age
(1)	(2)	(3)	(4)	(5)	(6)	(7)	(8)	(9)	(10)	(11)	(12)	(13)
		"	kpc	$W \text{ Hz}^{-1}$		GHz	nT	Myr		GHz	nT	Myr
J0139+3957	0.2107	370	1259	26.16	W	$16^{+4.3}_{-11.3}$	0.81	12^{+10}_{-1}	E	119^{+220}_{-116}	0.66	$5.3^{+29}_{-2.2}$
J0200+4049	0.0827	920	1414	25.34	W	$0.73^{+0.05}_{-0.20}$	0.20	143^{+25}_{-5}	E	$0.64^{+0.04}_{-0.17}$	0.18	151^{+25}_{-5}
J0807+7400	0.1204	555	1190	24.76	W	$5.0^{+27.7}_{-4.0}$	0.15	46^{+57}_{-28}	E	$2.8^{+5.6}_{-1.3}$	0.20	64^{+24}_{-27}

Table 5. Core flux densities of J0139+3957

Telescope	Resolution "	Date	Freq. MHz	S mJy	Ref.
(1)	(2)	(3)	(4)	(5)	(6)
GMRT	~ 10	2007 Jun 02	239	39.3 ± 6	P
GMRT	~ 10	2005 Jan 28	334	38.3 ± 6	P
GMRT	~ 5	2007 Jun 02	605	41.0 ± 4	P
GMRT	~ 5	2003 Aug 19	1287	35.0 ± 4	2
VLA	~ 5	1982 Sep	1465	33.0 ± 3	1
Cambridge	~ 5	1977 Oct	2695	24.0 ± 2	5
VLA	~ 15	2000 Jul 24	4841	12.0 ± 1	2
VLA	4.9	1989 Jul	4885	12.0 ± 1	4
VLA	~ 2	1977 Mar-May	4900	13.0 ± 2	6
Effelsberg	69	1990–1991	10550	4.0 ± 1	3

P: Present paper; 1: Gregorini et al. 1988; 2: Konar et al. 2004; 3: Mack et al. 1994; 4: Bondi et al. 1993; 5: Hine 1979; 6: Fomalont & Bridle 1978

**Figure 7.** The spectrum of the radio core of J0200+4049.

measurements are 143^{+25}_{-5} and 151^{+25}_{-5} Myr respectively (Table 4; Fig. 6), which are the largest amongst the three sources discussed here. More accurate measurements of the flux density at both low and high frequencies would help determine the break frequency more reliably. The lobes are relaxed with a depression in surface brightness in the western lobe. This clearly suggests that the lobes are no longer being fed with energy from the nucleus.

The core flux densities estimated by imaging with lower uv limits to minimise contamination by extended emission are listed in Table 6. Although the high-frequency spectrum appears to be fairly steep, with a spectral index of ~ 0.8 between 1289 and 4841 MHz, the spectrum appears to turn over at low frequencies (Fig. 7).

4.3 J0807+7400

This source is a giant low-power radio galaxy, the weakest of our three GRSs. Observations at 1.4 GHz by Lara et al. (2001) show a compact core component and a weak and extended halo-like emission elongated in the east-west direction with no evidence of either jets or hotspots. At 4.9 GHz, only the core component was visible. Lara et al. (2001) suggested that this object could be a relic FR II radio galaxy where hotspot regions are no longer present. Our GMRT images at low frequencies show the diffuse lobes and bridge of emission. The spectral ages of the lobes using our measurements are 46^{+57}_{-28} and 64^{+24}_{-27} Myr for the western and eastern lobes respectively (Table 4; Fig. 8).

The core has a flat spectral index at high frequencies but appears to have a steep radio spectrum with a spectral index of ~ 0.6 at lower frequencies (Fig. 9), possibly due to unresolved jet/lobe structure from more recent activity.

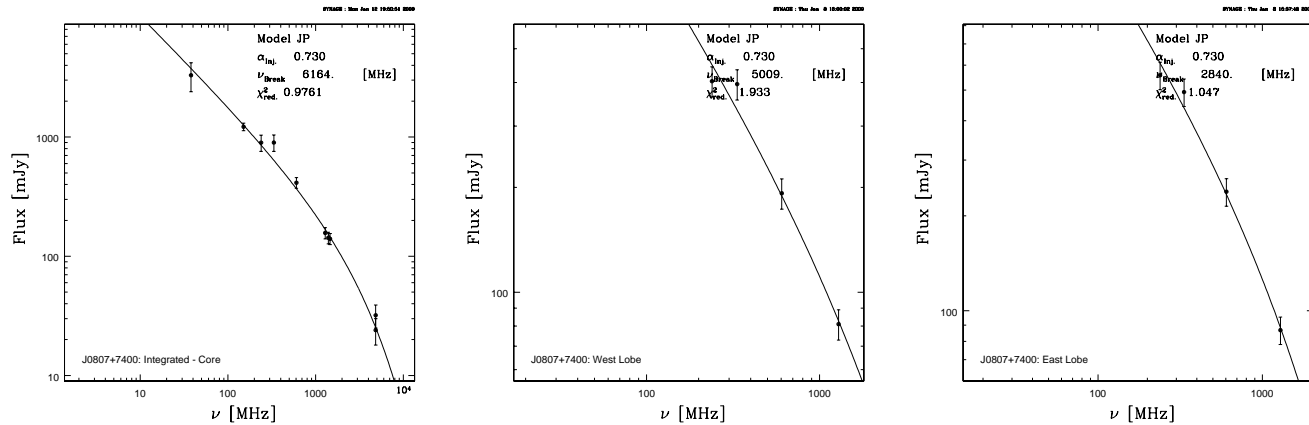
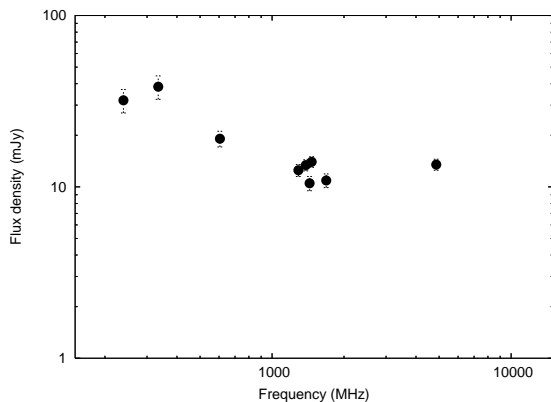
5 CONCLUDING REMARKS

We have presented low-frequency GMRT observations of the lobes of emission of three giant radio sources, J0139+3957, J0200+4049 and J0807+7400, with diffuse lobes of emission, but no hotspots and no jets from the nuclear region. Klein et al. (1995) had earlier suggested J0139+3957 to consist of relic lobes, while Lara et al. (2001) suggested that J0807+7400 is a relic FR II radio source. We have tried to explore this theme by examining the structure and spectra of all three sources over a large frequency range. Although these three sources do not have hotspots, their structures are not similar to the FRI sources which are characterised

Table 6. Core flux densities of J0200+4049

Teles-cope (1)	Resolution " (2)	Date (3)	Freq. MHz (4)	S mJy (5)	Ref. (6)
GMRT	~11	2007 Dec 29	239	7.6 ± 1.1	P
GMRT	~7	2004 Dec 25	333	9.5 ± 1.4	P
GMRT	~5	2007 Dec 29	605	9.2 ± 0.9	P
GMRT	~3	2004 Nov 25	1289	7.9 ± 0.8	P
VLA	~12	2000 Jul 24	4841	2.6 ± 0.3	1

P: Present paper; 1: Konar et al. 2004


Figure 8. The fits to the spectra of the entire source after subtracting the contribution of the core (left panel) as well as the western (middle panel) and eastern (right panel) lobes of J0807+7400 using the SYNAGE package.

Figure 9. The spectrum of the radio core of J0807+7400.

by jets that expand to form the diffuse lobes of emission. Also, the luminosities of two of the three sources are above the dividing line for these two classes of sources.

The spectral ages of the lobes estimated from SYNAGE fits to the spectra of the lobes, as well as their integrated spectra, are in the range of $\sim 5 \times 10^6$ to 1.5×10^8 yr, the upper range being close to time scales for which the lobes are likely to remain visible if not fed with a fresh supply of energy from the parent galaxy.

The structure and spectra suggest that these lobes are possibly no longer being fed, with one of the lobes in J0200+4049 exhibiting a depression in surface bright-

ness towards the centre of the lobe. However, all three have detected radio cores, two of which, J0139+3957 and J0200+4049, have spectra which flatten at lower frequencies, which could be indicative of an active core, while the core spectrum of J0807+7400 appears steep at low frequencies suggesting unresolved extended emission. The detection of cores suggests that their nuclei are currently active. Although these sources do not belong to the classic double-double radio galaxies, about a dozen or so of which are presently known (e.g. Saikia, Konar & Kulkarni 2006), these might also represent sources with evidence of episodic nuclear activity. It would be interesting to determine the structures of the cores from high-resolution radio observations. The relationship between the turnover frequency and source size for GPS objects (O’Dea 1998) shows that the source sizes are ~ 0.5 to 2 kpc for turnover frequencies of ~ 1 and 0.4 GHz respectively (see Figs. 5 and 7). Interpreting the cores as more recent activity, the time scales of episodic activity would range from $\sim 10^7$ to 10^8 yr.

ACKNOWLEDGMENTS

We thank an anonymous referee for helpful comments. The Giant Metrewave Radio Telescope is a national facility operated by the National Centre for Radio Astrophysics of the Tata Institute of Fundamental Research. We thank the staff for help with the observations. The National Radio Astronomy Observatory is a facility of the National Science Foundation operated under co-operative agreement by As-

Table 7. Core flux densities of J0807+7400

Teles- cope (1)	Resolution " (2)	Date (3)	Freq. MHz (4)	S mJy (5)	Ref. (6)
GMRT	~13	2005 Jan 07	239	32.0±5	P
GMRT	~9	2004 Dec 07	334	38.4±6	P
GMRT	~5	2005 Jan 07	605	19.1±2	P
GMRT	~3	2005 Jan 17	1289	12.5±1	P
VLA-B	~6	1995 Nov 19	1385	13.4±1	P
VLA-C	~14	1996 Feb 19	1685	10.9±1	P
VLA-D	~45	1993 Nov 01	1435	10.5±1	P
VLA-B+C	~12	1995 Nov 19	1465	14.0±1	1
VLA-C	~6	1996 Feb 19	1465		
VLA-C	~6	1996 Feb 19	4860	13.5±1	P

P: Present paper; 1: Lara et al. 2001

sociated Universities Inc. We thank the VLA staff for easy access to the archival data base. This research has made use of the NASA/IPAC extragalactic database (NED) which is operated by the Jet Propulsion Laboratory, Caltech, under contract with the National Aeronautics and Space Administration. We thank numerous contributors to the GNU/Linux group.

REFERENCES

- Baars J.W.M., Genzel R., Pauliny-Toth I.I.K., Witzel A., 1977, *A&A*, 61, 99
- Becker R.H., White R.L., Edwards A.L., 1991, *ApJS*, 75, 1
- Blundell K.M., Rawlings S., Willott C.J., 1999, *AJ*, 117, 677
- Bondi M., Gregorini L., Padrielli L., Parma P., 1993, *A&AS*, 101, 431
- Condon J.J., Cotton W.D., Greisen E.W., Yin Q.F., Perley R.A., Taylor G.B., Broderick J.J., 1998, *AJ*, 115, 1693
- Croston J.H., Hardcastle M.J., Harris D.E., Belsole E., Birkinshaw M., Worrall D.M., 2005, *ApJ*, 626, 733
- Falle S.A.E.G., 1991, *MNRAS*, 250, 581
- Fomalont E.B., Bridle A.H., 1978, *AJ*, 83, 725
- Gopal-Krishna, Wiita P.J., Saripalli L., 1989, *MNRAS*, 239, 173
- Gower J.F.R., Scott P.F., Wills D., 1967, *MemRAS*, 71, 49
- Gregory P.C., Condon J.J., 1991, *ApJS*, 75, 1011
- Gregorini L., Padrielli L., Parma P., Gilmore G., 1988, *A&AS*, 74, 107
- Gregorini L., Vigotti M., Mack K.-H., Zoenchen J., Klein U., 1998, *A&AS*, 133, 129
- Hales S.E.G., Mayer C.J., Warner P.J., Baldwin J.E., 1991, *MNRAS*, 251, 46
- Hales S.E.G., Baldwin J.E., Warner P.J., 1993, *MNRAS*, 263, 25
- Hales S.E.G., Waldram E.M., Rees N., Warner P.J., 1995, *MNRAS*, 274, 447
- Hine R.G., 1979, *MNRAS*, 189, 527
- Hardcastle M.J., Harris D.E., Worrall D.M., Birkinshaw M., 2004, *ApJ*, 612, 729
- Ishwara-Chandra C.H., Saikia D.J., 1999, *MNRAS*, 309, 100
- Jaffe W.J., Perola G.C., 1973, *A&A*, 26, 423
- Jamroz M., Konar C., Machalski J., Saikia D.J., 2008, *MNRAS*, 385, 1286
- Jeyakumar S., Wiita P.J., Saikia D.J., Hooda J.S., 2005, *A&A*, 432, 823
- Kaiser C.R., Alexander P., 1997, *MNRAS*, 286, 215
- Kaiser C.R., Alexander P., 1999, *MNRAS*, 302, 515
- Klein U., Mack K.-H., Gregorini L., Parma P., 1995, *A&A*, 303, 427
- Konar C., Saikia D.J., Ishwara-Chandra C.H., Kulkarni V.K., 2004, *MNRAS*, 355, 845
- Konar C., Jamroz M., Saikia D.J., Machalski J., 2008, *MNRAS*, 383, 525
- Lara L., Cotton W.D., Feretti L., Giovannini G., Marcaide J.M., Márquez I., Venturi T., 2001, *A&A*, 370, 409
- Leahy J.P., Muxlow T.W.B., Stephens P.W., 1989, *MNRAS*, 239, 401
- Liu R., Pooley G., Riley J.M., 1992, *MNRAS*, 257, 545
- Machalski J., Chyży K.T., Stawarz L., Koziel D., 2007, *A&A*, 462, 43
- Machalski J., Koziel-Wierzbowska D., Jamroz M., Saikia D.J., 2008, *ApJ*, 679, 149
- Mack K.-H., Gregorini L., Parma P., Klein U., 1994, *A&AS*, 103, 157
- Mack K.-H., Klein U., O’Dea C. P., Willis A. G., Saripalli L., 1998, *A&A*, 329, 431
- Murgia M., 1996, Laurea Thesis, University of Bologna
- Murgia M., Fanti C., Fanti R., Gregorini L., Klein U., Mack K.-H., Vigotti M., 1999, *A&A*, 345, 769
- O’Dea C.P., 1998, *PASP*, 110, 493
- Pilkington J.D.H., Scott P.F., 1965, *MemRAS*, 69, 183
- Saikia D.J., Konar C., Kulkarni V.K., 2006, *MNRAS*, 366, 1391
- Saripalli L., Patnaik A.R., Porcas R.W., Graham D.A., 1997, *A&A*, 328, 78
- Schoenmakers A.P., Mack K.-H., de Bruyn A.G., Röttgering H.J.A., Klein U., van der Laan H., 2000, *A&AS*, 146, 293
- Schoenmakers A.P., de Bruyn A.G., Röttgering H.J.A., van der Laan H., 2001, *A&A*, 374, 861
- Spergel D.N. et al., 2003, *ApJS*, 148, 175
- Subrahmanyan R., Saripalli L., 1993, *MNRAS*, 260, 908
- Subrahmanyan R., Saripalli L., Hunstead R.W., 1996, *MNRAS*, 279, 257
- Vigotti M., Grueff G., Perley R., Clark B.G., Bridle A.H., 1989, *AJ*, 98, 419
- Vigotti M., Gregorini L., Klein U., Mack K.-H., 1999, *A&AS*, 139, 359
- Viner M.R., Erickson W.C., 1975, *AJ*, 80, 931
- White R.L., Becker R.H., 1992, *ApJS*, 79, 331